

Temperature-pressure phase diagram of the superconducting iron pnictide LiFePK. Mydeen,^{1,*} E. Lengyel,¹ Z. Deng,² X. C. Wang,² C. Q. Jin,² and M. Nicklas^{1,†}¹Max Planck Institute for Chemical Physics of Solids, 01187 Dresden, Germany²Institute of Physics, Chinese Academy of Sciences, Beijing, China

(Received 3 March 2010; revised manuscript received 5 May 2010; published 13 July 2010)

Electrical-resistivity and magnetic-susceptibility measurements under hydrostatic pressure up to $p \approx 2.75$ GPa have been performed on superconducting (SC) LiFeP. A broad SC region exists in the temperature-pressure (T - p) phase diagram. No indications for a spin-density-wave transition have been found, but an enhanced resistivity coefficient at low pressures hints at the presence of magnetic fluctuations. Our results show that the SC state in LiFeP is more robust than in the isostructural and isoelectronic LiFeAs. We suggest that this finding is related to the nearly regular $[\text{FeP}_4]$ tetrahedron in LiFeP.

DOI: 10.1103/PhysRevB.82.014514

PACS number(s): 74.70.Xa, 74.62.Fj, 74.25.Dw

I. INTRODUCTION

The recently discovered iron-based superconductors attract a great deal of interest because of their high critical temperatures up to $T_c = 55$ K.¹⁻⁷ Soon after the discovery of superconductivity in the iron- and nickel-based oxyphosphides, LaFePO (Ref. 1) and LaNiPO,² superconductivity was found in LaFeAsO_{0.89}F_{0.11} (“1111” type) with a critical temperature of about 26 K.³ Furthermore, the application of hydrostatic pressure leads to an increase in T_c up to 43 K at about 4 GPa.⁸ The superconductivity in iron-pnictide compounds is closely related to their layered structure, where the iron-pnictide layers are interlaced with charge-reservoir layers. Electron or hole doping, both inside and outside of the iron-pnictide layers, strongly affects the superconducting (SC) properties.

The effect of external pressure on the structural and electronic properties of the iron-based superconductors can be subtle. In LaFeAsO_{1-x}F_x and SmFeAsO_{1-x}F_x the application of pressure revealed an anisotropic lattice compressibility at low pressures,⁹ which results in a significant modification of electronic density of states (DOS). In optimally doped LaFeAsO_{1-x}F_x T_c decreases linearly with increasing pressure up to 30 GPa. This decrease is accompanied by the lattice properties becoming less anisotropic.¹⁰ The close connection between structural properties and superconductivity is further shown in $Re\text{FeAsO}_{1-\delta}$ (Re =rare-earth metal). Here, T_c attains its maximum value where the $[\text{FeAs}_4]$ units form a regular tetrahedron.^{11,12} In Ba(Fe_{0.92}Co_{0.08})₂As₂ (“122” type) the uniaxial pressure dependencies of T_c are highly anisotropic and quite pronounced.¹³ T_c is anticipated to increase with increasing c/a ratio.

Superconductivity was reported in the “111”-type materials LiFeAs (Refs. 14–16) and NaFeAs.¹⁷ In contrast to “1111” and “122” compounds and to the isostructural NaFeAs no signature of a spin-density wave (SDW) or structural transition has been observed in LiFeAs regardless of having a similar charge density in the FeAs layers.^{18–21} Recently, superconductivity below 6 K was discovered in the As free “111” compound LiFeP,^{22,23} which is isostructural and isoelectronic to LiFeAs and can be considered as compressed LiFeAs. The occurrence of bulk superconductivity in both stoichiometric LiFeAs and LiFeP makes them special

among the iron-pnictide materials. Usually in stoichiometric “1111” and “122” type compounds the application of external pressure or doping is needed to induce bulk superconductivity. External pressure and isoelectronic chemical substitution have a different effect on the crystal structure.^{22,24} This allows for a detailed study of the influence of structural properties on superconductivity. In this paper we study the effect of hydrostatic pressure on LiFeP by electrical resistivity (ρ) and magnetic susceptibility (χ_{ac}) experiments.

II. EXPERIMENTAL DETAILS

LiFeP polycrystals were synthesized as described in Ref. 22. We carried out four-probe electrical resistivity and ac-susceptibility measurements under hydrostatic pressure using a physical property measurement system (PPMS, Quantum Design) and a commercial flow cryostat, respectively, utilizing a LR700 resistance/mutual inductance bridge (Linear Research). A compensated coil system placed outside of the pressure cell was used for the ac-susceptibility experiments. Pressures up to 2.75 GPa were generated using a double-layer piston-cylinder-type pressure cell. Silicone fluid served as pressure transmitting medium. The pressure was determined at low temperatures by monitoring the pressure-induced shift of the SC transition temperature of Pb placed close to the sample. The narrow width of the transition $\Delta T \leq 12$ mK, corresponding to a pressure gradient $\Delta p \leq 0.032$ GPa, at all pressures confirmed the good hydrostatic-pressure conditions inside the cell.

III. EXPERIMENTAL RESULTS

The temperature dependence of the electrical resistivity of LiFeP at three representative pressures is depicted in Fig. 1. In the normal state $\rho(T)$ exhibits a good metallic behavior with no evidence for a SDW instability which is found in many of “1111”- or “122”-type iron-pnictide materials. A residual resistivity ratio $RRR = \rho_{300\text{ K}} / \rho_0 \approx 43$ at atmospheric pressure confirms the good quality of our polycrystalline sample. Here, $\rho_{300\text{ K}}$ is the resistivity at 300 K and ρ_0 the residual resistivity. At low temperatures, a sharp decrease in $\rho(T)$ to zero marks the onset of superconductivity, which is

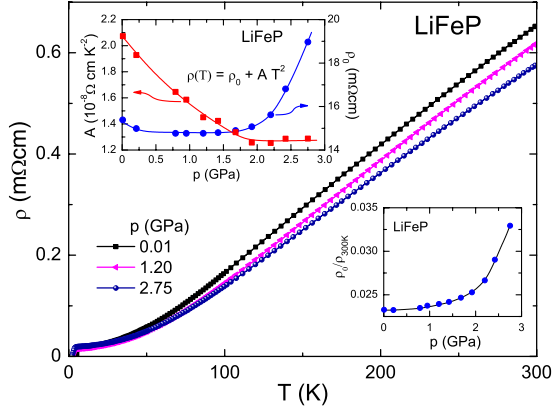


FIG. 1. (Color online) Electrical resistivity, $1.8 \leq T \leq 300$ K, of LiFeP for three representative pressures. The upper inset depicts the pressure dependence of the residual resistivity ρ_0 and the prefactor A obtained from a fit of $\rho(T) = \rho_0 + AT^2$ to the low- T normal-state resistivity. Details are given in the text. The lower inset displays the pressure dependence of the ratio $\rho_0/\rho_{300\text{ K}}$, where $\rho_{300\text{ K}}$ is the resistivity at $T=300$ K.

observed in the whole investigated pressure range ($p \leq 2.75$ GPa). The low- T normal-state resistivity follows a T^2 dependence at all pressures indicating a Fermi-liquid state. The pressure dependence of the parameters ρ_0 and A of a $\rho(T) = \rho_0 + AT^2$ fit to the data ($T_c \leq T \leq 15$ K) is presented in the upper inset of Fig. 1. The observation of a T^2 behavior at such elevated temperatures hints at the presence of strong electronic correlations. The temperature coefficient A is a measure of the quasiparticle-quasiparticle (QP-QP) scattering rate. $A(p)$ decreases by a factor of 1.6 from atmospheric pressure to $p=2$ GPa and stays constant with further increasing pressure, indicating a reduction in the QP-QP scattering rate for $p \leq 2$ GPa. The enhanced QP-QP scattering rate at low pressures might be a hint for the presence of spin fluctuations and indicate the proximity of LiFeP to magnetic order at ambient pressure despite no direct evidence for long-range magnetic order has been found neither in LiFeP nor in its homologue LiFeAs.

At ambient pressure, we find the onset of the resistive transition at about ≈ 6 K in good agreement with the literature.²² Further on, we will use the $\rho(T)=0$ criterion to define T_c from our resistivity data. With increasing pressure the SC transition shifts to lower temperatures (see Fig. 2). The width of the transition is nearly pressure independent up to $p \approx 2.25$ GPa, even though the onset becomes more rounded before a noticeable broadening becomes evident. The significant broadening is accompanied by an increase in the low-temperature normal-state resistivity, which is basically pressure independent below $p \approx 2$ GPa. This behavior is intrinsic to the sample and not caused by, e.g., cracks in the sample, since the room-temperature resistivity, $\rho_{300\text{ K}}(p)$, decreases monotonously upon increasing pressure. This is also evidenced by the strong increase in the ratio $\rho_0(p)/\rho_{300\text{ K}}(p)$ (see lower inset in Fig. 1).

In addition to $\rho(T)$ we measured $\chi_{ac}(T)$ on the same sample and at the same pressures. $\chi_{ac}(T)$ exhibits a narrow, steplike feature at the SC transition. $\rho(T)$ reaches zero right

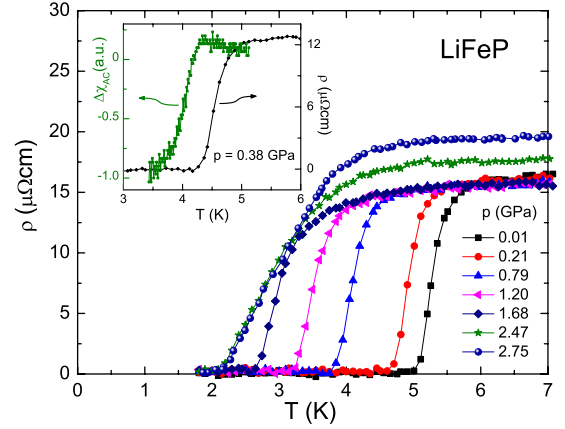


FIG. 2. (Color online) Low-temperature electrical resistivity of LiFeP as function of temperature for different pressures as indicated. The inset displays the ac susceptibility and the electrical resistivity at $p=0.38$ GPa in the temperature region around the SC transition.

at the temperature where $\chi_{ac}(T)$ exhibits the onset of the diamagnetic response. Above $p=0.79$ GPa, T_c drops out of our measurement window for χ_{ac} . The inset of Fig. 2 shows $\chi_{ac}(T)$ and, for comparison, $\rho(T)$ at $p=0.38$ GPa. The evolution of T_c with increasing p is depicted in Fig. 3. The narrow width of the SC transition in resistivity and, further, the good correspondence between T_c determined by the $\rho(T)$ and the $\chi_{ac}(T)$ experiments in the T - p phase diagram is unusual for superconductivity in stoichiometric “1111” and “122” materials. There, quite often zero resistance is found without any indication for bulk superconductivity or a very broad transition is observed (e.g., Refs. 26 and 27). We further note that we do not find any indication for grain-boundary effects on the SC transition. In that case two SC transition temperatures, one corresponding to intragrain and another corresponding to intergrain superconducting transi-

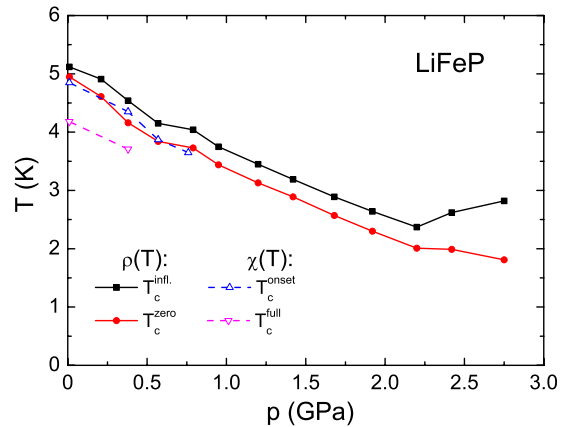


FIG. 3. (Color online) Temperature-pressure phase diagram of LiFeP. The solid symbols correspond to results from $\rho(T)$ measurements. $T_c^{\text{infl.}}$ is defined by the inflection point of $\rho(T)$ and T_c^{zero} by the temperature where zero resistivity is obtained. The open symbols correspond to T_c determined by $\chi_{ac}(T)$ experiments. T_c^{onset} marks the onset of the diamagnetic response and T_c^{full} the full transition.

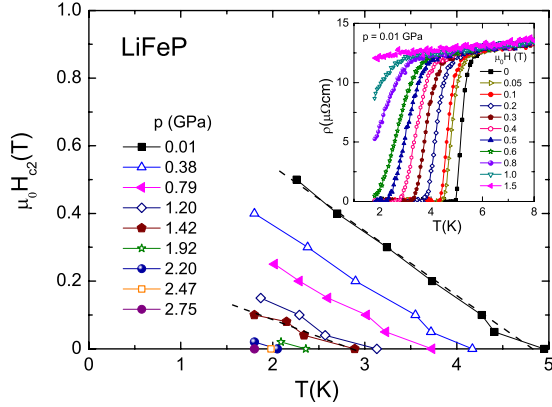


FIG. 4. (Color online) Magnetic field-temperature phase diagram of LiFeP for different pressures. The dashed lines at $p=0.01$ and 1.42 GPa are serving as an example of the linear fits to the data. The inset shows the resistivity data for $p=0.01$ GPa for different magnetic fields. The zero-resistivity criterion was used for determining T_c .

tions would be expected in $\rho(T)$, as well as in $\chi_{ac}(T)$, which we clearly do not observe.

To determine the SC upper-critical field, $H_{c2}(T)$, we conducted measurements of the electrical resistivity in magnetic fields. H_{c2} vs T curves at different pressures are displayed in Fig. 4. $H_{c2}(T)$ exhibits a roughly linear temperature dependence in the accessible temperature range ($T \geq 1.8$ K) with the exception of the first data point in magnetic field ($\mu_0 H = 0.5$ T), which indicates the presence of a small tail. A similar tail has been previously reported in other iron-based superconductors.^{28–30} As possible origin of the tail multiband effects were discussed. Increasing pressure suppresses $H_{c2}(T)$ effectively and, correspondingly, the absolute value of the slope $\mu_0 dH_{c2}(T)/dT$ of a straight-line fit to the data decreases from 1.92 T/K at 0.01 GPa to 0.95 T/K at 1.42 GPa. Furthermore, with increasing magnetic field the SC transition in $\rho(T)$ gradually broadens as shown for $p = 0.01$ GPa in the inset of Fig. 4. The broadening of the resistive transition on increasing magnetic field indicates an anisotropy of $H_{c2}(T)$ as anticipated for a quasi-two-dimensional electronic structure.³¹

IV. DISCUSSION

In comparison with LiFeAs, LiFeP can be viewed as *compressed* LiFeAs. At 5.5 – 6.5 GPa T_c of LiFeAs becomes comparable with T_c of LiFeP at atmospheric pressure: LiFeAs “becomes” LiFeP.³² The lattice parameters obtained for LiFeP are $a=3.692$ Å, $c=6.031$ Å (Ref. 22) compared to $a=3.670$ Å, $c=6.108$ Å for LiFeAs at 6.54 GPa.²⁴ The lattice parameters a and c in LiFeAs are contracted by 2.7% and 3.9% , respectively, at 6.54 GPa, whereas the replacement of As by P reveals a highly anisotropic contraction of a and c by 2.1% and 5.1% , respectively. This leads to a smaller structural anisotropy in LiFeP compared to LiFeAs at 6.54 GPa. It has been pointed out for the iron-pnictides that T_c attains maximum values when the $[\text{FePn}_4]$, where $\text{Pn}=\text{P}$, As, form a regular tetrahedron.^{11,12} At ambient pressure the

$[\text{FeP}_4]$ tetrahedron of LiFeP is only slightly distorted with $\alpha=108.58^\circ$ and $\beta=109.92^\circ$ (Ref. 22) while LiFeAs at 6.54 GPa possesses a highly distorted tetrahedron $\alpha=99.39^\circ$ and $\beta=114.70^\circ$.²⁴ The bond angle of a regular tetrahedron is 109.47° . A nearly perfect $[\text{FeP}_4]$ tetrahedron in LiFeP but a highly distorted $[\text{FeAs}_4]$ tetrahedron in LiFeAs and taking into account a similar T_c in both materials suggest that the perfectness of the $[\text{FePn}_4]$ tetrahedron is not the determining property for the value of T_c . Moreover, our result suggests that changes in the DOS other than those strictly related to the perfectness of the $[\text{FePn}_4]$ tetrahedron are governing the value of T_c . However, our experiments reveal that superconductivity in LiFeP is less sensitive to pressure than in LiFeAs. In LiFeAs $T_c(p)$ decreases linearly on increasing pressure in the whole pressure range up to ~ 10 GPa.²⁵ The initial slope of $T_c(p)$, $|dT_c(p)/dp|_{p=0}=1.23$ K/GPa, for LiFeP is significantly smaller compared to the value in LiFeAs, $|dT_c(p)/dp|_{p=0}=(1.56-2)$ K/GPa.^{24,33} Since $T_c(p)$ decreases linearly in LiFeAs, the same significant difference in the slopes of $T_c(p)$ is present when we compare them where the T_c 's of LiFeP at $p=0$ and LiFeAs under pressure (5.5 – 6.5 GPa) are matching. This clearly indicates that considering the same T_c superconductivity in LiFeP is more stable than in LiFeAs. This is furthermore supported by a decreasing slope of $T_c(p)$ upon increasing pressure in LiFeP (see Fig. 3). Therefore, our study suggests that a more regular $[\text{FePn}_4]$ tetrahedron “strengthens” the SC state, but is not determining the size of T_c .

We will now turn to the unusual increase in the low- T normal-state resistivity above $p \approx 2$ GPa. While the residual resistivity, $\rho_0(p)$, increases by about $1/3$ from 1.68 GPa to 2.75 GPa, the A coefficient stays nearly pressure independent in this pressure range. This indicates that the QP-QP scattering rate does not change, but additional contributions to the residual scattering appear and become stronger upon increasing pressure. Since, as we discussed before, $\rho_{300\text{K}}(p)$ decreases in the mentioned pressure range and, thus, we can exclude an extrinsic reason and, clearly, pressure does not add impurities, a different scattering mechanism has to be considered. An increase in $\rho_0(p)$ is generally caused by additional disordered scattering centers. A similar increase in the resistivity at low temperatures is observed in LiFeAs, but at much higher pressures $p \geq 11$ GPa.²⁵ There, it has been proposed that additional disordered scattering centers created by local magnetic ordering cause the enhanced ρ_0 .²⁵ Increasing pressure reduces the in-plane Fe-Fe distance and concomitantly enhances local magnetic correlations leading to additional magnetic scattering centers.

V. CONCLUSION

In summary, we have studied the T - p phase diagram of the iron-pnictide superconductor LiFeP. Our experiments evidence a more robust SC state than in the isostructural homologue LiFeAs. We relate this to the nearly regular $[\text{FePn}_4]$ tetrahedron in LiFeP in contrast to the highly distorted one in LiFeAs. However we do not find a general relationship of the bond angle α and T_c as suggested in

literature.¹¹ Furthermore, we observe an enhanced QP-QP scattering rate at low pressures, which might indicate the presence of spin fluctuations. However further studies are needed to verify this speculation.

ACKNOWLEDGMENT

We thank the Deutsche Forschungsgemeinschaft (DFG) for financial support through SPP 1458.

*kamal@cpfs.mpg.de

†nicklas@cpfs.mpg.de

- ¹Y. Kamihara, H. Hiramatsu, M. Hirano, R. Kawamura, H. Yanagi, T. Kamiya, and H. Hosono, *J. Am. Chem. Soc.* **128**, 10012 (2006).
- ²T. Watanabe, H. Yanagi, T. Kamiya, Y. Kamihara, H. Hiramatsu, M. Hirano, and H. Hosono, *Inorg. Chem.* **46**, 7719 (2007).
- ³Y. Kamihara, T. Watanabe, M. Hirano, and H. Hosono, *J. Am. Chem. Soc.* **130**, 3296 (2008).
- ⁴X. H. Chen, T. Wu, G. Wu, R. H. Liu, H. Chen, and D. F. Fang, *Nature (London)* **453**, 761 (2008).
- ⁵G. F. Chen, Z. Li, D. Wu, G. Li, W. Z. Hu, J. Dong, P. Zheng, J. L. Luo, and N. L. Wang, *Phys. Rev. Lett.* **100**, 247002 (2008).
- ⁶Z. A. Ren, J. Yang, W. Lu, W. Yi, G. C. Che, X. L. Dong, L. L. Sun, and Z. X. Zhao, *Mater. Res. Innovations.* **12**, 105 (2008).
- ⁷A. S. Sefat, M. A. McGuire, B. C. Sales, R. Jin, J. Y. Howe, and D. Mandrus, *Phys. Rev. B* **77**, 174503 (2008).
- ⁸H. Takahashi, K. Igawa, K. Arii, Y. Kamihara, M. Hirano, and H. Hosono, *Nature (London)* **453**, 376 (2008).
- ⁹H. Takahashi, H. Okada, K. Igawa, Y. Kamihara, M. Hirano, H. Hosono, K. Matsubayashi, and Y. Uwatoko, *J. Supercond. Novel Magn.* **22**, 595 (2009).
- ¹⁰G. Garbarino, P. Toulemonde, M. Álvarez-Murga, A. Sow, M. Mezouar, and M. Núñez-Regueiro, *Phys. Rev. B* **78**, 100507(R) (2008).
- ¹¹C.-H. Lee, A. Iyo, H. Eisaki, H. Kito, M. T. Fernandez-Diaz, T. Ito, K. Kihou, H. Matsuhata, M. Braden, and K. Yamada, *J. Phys. Soc. Jpn.* **77**, 083704 (2008).
- ¹²J. Zhao, L. Wang, D. Dong, Z. Liu, H. Liu, G. Chen, D. Wu, J. Luo, N. Wang, Y. Yu, C. Jin, and Q. Guo, *J. Am. Chem. Soc.* **130**, 13828 (2008).
- ¹³F. Hardy, P. Adelman, T. Wolf, H. v. Löhneysen, and C. Meingast, *Phys. Rev. Lett.* **102**, 187004 (2009).
- ¹⁴X. C. Wang, Q. Q. Liu, Y. X. Lv, W. B. Gao, L. X. Yang, R. C. Yu, F. Y. Li, and C. Q. Jin, *Solid State Commun.* **148**, 538 (2008).
- ¹⁵M. J. Pitcher, D. R. Parker, P. Adamson, S. J. C. Herkelrath, A. T. Boothroyd, R. M. Ibberson, M. Brunelli, and S. J. Clarke, *Chem. Commun. (Cambridge)* **2008**, 5918.
- ¹⁶J. H. Tapp, Z. Tang, B. Lv, K. Sasmal, B. Lorenz, P. C. W. Chu, and A. M. Guloy, *Phys. Rev. B* **78**, 060505(R) (2008).
- ¹⁷D. R. Parker, M. J. Pitcher, P. J. Baker, I. Franke, T. Lancaster, S. J. Blundell, and S. J. Clarke, *Chem. Commun. (Cambridge)* **2009**, 2189.
- ¹⁸C. de la Cruz, Q. Huang, J. W. Lynn, J. Y. Li, W. Ratcliff II, J. L. Zarestky, H. A. Mook, G. F. Chen, J. L. Luo, N. L. Wang, and P. C. Dai, *Nature (London)* **453**, 899 (2008).
- ¹⁹A. I. Goldman, D. N. Argyriou, B. Ouladdiaf, T. Chatterji, A. Kreyssig, S. Nandi, N. Ni, S. L. Bud'ko, P. C. Canfield, and R. J. McQueeney, *Phys. Rev. B* **78**, 100506(R) (2008).
- ²⁰A. Jesche, N. Caroca-Canales, H. Rosner, H. Borrmann, A. Ormeci, D. Kasinathan, H. H. Klauss, H. Luetkens, R. Khasanov, A. Amato, A. Hoser, K. Kaneko, C. Krellner, and C. Geibel, *Phys. Rev. B* **78**, 180504(R) (2008).
- ²¹M. Rotter, M. Tegel, D. Johrendt, I. Schellenberg, W. Hermes, and R. Pöttgen, *Phys. Rev. B* **78**, 020503(R) (2008).
- ²²Z. Deng, X. C. Wang, Q. Q. Liu, S. J. Zhang, Y. X. Lv, J. L. Zhu, R. C. Yu, and C. Q. Jin, *EPL* **87**, 37004 (2009).
- ²³J.-T. Han, J.-S. Zhou, J.-G. Cheng, and J. B. Goodenough, *J. Am. Chem. Soc.* **132**, 908 (2010).
- ²⁴M. Mito, M. J. Pitcher, W. Crichton, G. Garbarino, P. J. Baker, S. J. Blundell, P. Adamson, D. R. Parker, and S. J. Clarke, *J. Am. Chem. Soc.* **131**, 2986 (2009).
- ²⁵S. J. Zhang, X. C. Wang, R. Sammynaiken, J. S. Tse, L. X. Yang, Z. Li, Q. Q. Liu, S. Desgreniers, Y. Yao, H. Z. Liu, and C. Q. Jin, *Phys. Rev. B* **80**, 014506 (2009).
- ²⁶S. R. Saha, N. P. Butch, K. Kirshenbaum, J. Paglione, and P. Y. Zavalij, *Phys. Rev. Lett.* **103**, 037005 (2009).
- ²⁷M. Kumar, M. Nicklas, A. Jesche, N. Caroca-Canales, M. Schmitt, M. Hanfland, D. Kasinathan, U. Schwarz, H. Rosner, and C. Geibel, *Phys. Rev. B* **78**, 184516 (2008).
- ²⁸Z.-S. Wang, H.-Q. Luo, C. Ren, and H.-H. Wen, *Phys. Rev. B* **78**, 140501(R) (2008).
- ²⁹F. Hunte, J. Jaroszynski, A. Gurevich, D. C. Larbalestier, R. Jin, A. S. Sefat, M. A. McGuire, B. C. Sales, D. K. Christen, and D. Mandrus, *Nature (London)* **453**, 903 (2008).
- ³⁰C. F. Miclea, M. Nicklas, H. S. Jeevan, D. Kasinathan, Z. Hosain, H. Rosner, P. Gegenwart, C. Geibel, and F. Steglich, *Phys. Rev. B* **79**, 212509 (2009).
- ³¹S. Lebègue, *Phys. Rev. B* **75**, 035110 (2007).
- ³² T_c of LiFeAs has been extrapolated linearly to higher pressures using $T_c(p)$ determined from $\chi_{ac}(T)$ reported in Refs. 24 and 33 [in the same way as we have determined $T_c(p)$ in LiFeP].
- ³³M. Gooch, B. Lv, J. H. Tapp, Z. Tang, B. Lorenz, A. M. Guloy, and P. C. W. Chu, *EPL* **85**, 27005 (2009).